Helicon–Drift-Current Interaction in a Solid-State Plasma Waveguide

C. NANNEY
Bell Telephone Laboratories, Murray Hill, New Jersey
(Received 18 September 1964; revised manuscript received 30 December 1964)

Theoretical predictions indicate that a drift current in a single-component plasma should produce a Doppler-type shift in the helicon-wave velocity. In this paper we report the observation of such an interaction between a traveling helicon wave in a solid-state plasma waveguide and a drift current in the same plasma. The wave-current interaction was observed for frequencies in the low megacycle range. The plasma waveguide was a bar of n-type PbTe at 1.8°K through which dc drift-current densities up to 2500 A/cm^2 were passed. The observed interaction is in reasonably good agreement with theory, provided waveguide and damping effects are taken into account. Waveguide effects are shown to reduce the magnitude of the interaction. Collision damping of the helicons complicates the interpretation of the data by introducing an apparent asymmetry into the measured effect of the drift current for directions parallel and antiparallel to the helicon propagation direction.

I. INTRODUCTION

RECENTLY, Bok and Nozieres[1] derived an expression for the interaction of transverse electromagnetic waves with a drifting electron-hole plasma. They predict an amplifying instability with sufficiently large drift velocities and a Doppler-type interaction for small velocities. This theory was found to explain the effect observed by Bartelink[2] of a drift current on the polarization of damped Alfven waves in the electron-hole plasma of bismuth. The theory, applied to a single species of mobile charge carrier, also predicts a Doppler-type interaction but no instability.

The theory for a transverse electromagnetic wave of radial frequency ω and wave vector $\mathbf{k}$, propagating in an infinite drifting, single-component plasma in a magnetic field ($\mathbf{k}\|\mathbf{B}\|\mathbf{v}_D$), predicts a dielectric constant given by

$$\epsilon(\omega,k)=\frac{c^2k^2}{\omega^2}=\epsilon_l-\frac{i\tau\omega_p^2(1-\mathbf{k}\cdot\mathbf{v}_D/\omega)}{\omega[-1+i(\omega\pm\omega_c)\tau]}, \quad (1)$$

where ϵ_l is the lattice dielectric constant, ω_p is the plasma frequency, v_D is the drift velocity, ω_c is the cyclotron frequency and τ is the relaxation time. The rest of the symbols have their usual significance. Equation (1) is identical to the undrifted plasma except for the $\mathbf{k}\cdot\mathbf{v}_D$ term on the right. This term arises from the $\mathbf{v}_D\times\mathbf{B}_{rf}$ term of the Lorentz force equation. Equation (1) is valid in the local limit, that is, $kv_F\ll\omega_c$, where v_F is the Fermi velocity. This inequality is well satisfied in the present experiment. Solving Eq. (1) with typical helicon conditions $\omega\ll\omega_c$, $\omega_c\tau\gg1$, $|\epsilon|\gg\epsilon_l$, we obtain an expression for the helicon phase velocity ω/k as a function of the drift velocity, v_D:

$$\frac{\omega}{k}=\tfrac{1}{2}[v_D\pm(4v_H^2+v_D^2)^{1/2}] \quad (2a)$$

$$\simeq\pm v_H+\tfrac{1}{2}v_D \quad v_D\ll v_H, \quad (2b)$$

where $v_H=(H\omega/Ne)^{1/2}$ is the helicon phase velocity in the absence of a drift current.[3] Equation (2a) shows clearly that it is not possible to match the drift velocity to the helicon phase velocity in a single-component plasma. Consequently, no amplification of helicon waves is expected in a single-component plasma.

In the next section, the experimental arrangement employed in this experiment is discussed. Section III discusses the helicon dispersion relation in a waveguide. A comparison is made between the theoretical and the experimentally determined dispersion relations. Section IV reports the observation of an interaction between lightly damped, traveling helicon waves and a drift current in a solid-state plasma which forms a waveguide structure.

II. EXPERIMENTAL

In this experiment we employ an arrangement specifically designed to study *traveling* helicon waves in a solid-state plasma waveguide. A schematic diagram of the system is shown in the inset of Fig. 1. The sample is a bar of n-type PbTe, typically 1.7×1.7×12 mm^3, with current leads attached to the ends. (PbTe was chosen for its very high mobility, $\mu\simeq10^6$ cm^2/V-sec at helium temperatures, and its relatively high carrier concentration.) The static magnetic field B is parallel to the bar axis and may have for measurement purposes

[1] J. Bok and P. Nozieres, J. Chem. Phys. Solids 24, 709 (1963).
[2] D. J. Bartelink, Phys. Rev. Letters 12, 470 (1964). D. J. Bartelink, Symposium on Plasma Effects in Solids, Paris 1964 (unpublished).

[3] The physical explanation for the factor of ½ multiplying the drift velocity of the plasma in Eq. (2b) lies in the dispersive nature of the helicon waves in a plasma. If a light wave is traveling in a moving nondispersive dielectric, the change in the observed velocity of the wave is just equal to the velocity of the medium, provided $v\ll c$. However, the velocity of the helicons depends (strongly) on the frequency; and the frequency itself depends on velocity. Consequently, the velocity must be specified for a particular value of the frequency; the correct value of ω is that in the rest system of the medium. [See for example: C. Moller, *The Theory of Relativity* (Oxford University Press, London, 1952), p. 63.] This gives rise to an additional term in Doppler-shifted velocity, which is just $v_D\omega n^{-1}dn/d\omega$, where n is the index of refraction. For most dielectrics this term is of the order of a few percent; however, for the highly dispersive helicon medium this term is large and equal to $-\frac{1}{2}$. This gives rise to the interesting possibility of a wave having a zero Doppler shift in velocity if its velocity is linear in frequency.

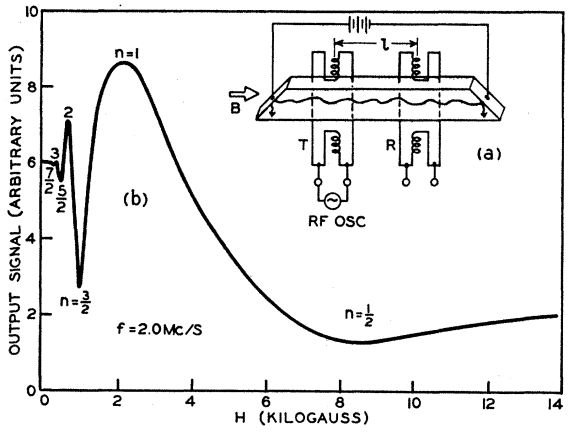

FIG. 1. (a) A schematic drawing of the sample showing the coil arrangement. (b) A curve of helicon transmission as a function of magnetic field. The sample (N-4) is a bar of n-type PbTe at 4.2°K, with a concentration of $n=2.8\times10^{17}$/cc. The bar dimensions are $1.7\times1.7\times11.5$ mm³ and $l=3.58$ mm. The maxima and minima are labeled according to the number of wavelengths in the length l.

a small low-frequency modulation component b_{ac}. Two pairs of small coils are arranged on opposite sides of the bar, separated by a distance l. Opposite coils are connected in parallel. The coils are typically 0.7 mm in diameter and have 20 turns of No. 44 Cu wire. Smaller diameter coils were found very inefficient for coupling the signal into or out of the sample. One pair of coils T is connected to an amplitude-modulated radio-frequency oscillator and excites the helicon wave in the bar. The other pair R couples the signal out of the bar into a communications recevier for rf demodulation. The audio-signal output of the receiver is fed into a phase-sensitive detector, which may be locked onto either the rf modulation frequency or the magnetic-field modulation frequency. The output of the detector is plotted versus magnetic field on an x-y recorder, showing the helicon transmission in the first case and the derivative of the transmission in the latter.

The end faces of the solid waveguide are cut at 45° with respect to the guide axis and the external magnetic field, in order to assist in assuring a single traveling wave from T to R. Waves which are traveling parallel to the bar axis are reflected at the ends so as to propagate nearly perpendicular to the magnetic field. The reflected waves are more strongly attenuated than would be waves reflected from a surface normal to the magnetic field, since the attenuation increases as the angle between the propagation vector and the field increases. (Helicons do not propagate perpendicular to the magnetic field.) It is not possible to obtain reflection exactly perpendicular to the external field due to the anisotropic nature of the plasma and the fact that a finite wavelength precludes a propagation vector parallel to the guide axis. Nevertheless, the effective damping will be appreciably greater than if the end faces were orthogonal to the guide axis. In addition, the solder contacts covering the end faces were found to be strongly absorbing. The experimental transmission curves in almost all cases indicated a pure traveling wave free from resonances.

Figure 1(b) shows a typical plot of the transmission as a function of magnetic field in a sample of n type PbTe ($N=2.8\times10^{17}$/cm³) at 1.8°K. This curve is interpreted as an interference[4] between the helicon waves and the constant, reactively coupled leakage signal from T to R. At each maximum the signal coupled out of the bar interferes constructively with the leakage signal. The helicon signal is phase-shifted by $2\pi n$ rad, compared to the input signal, as a result of its being propagated as a slow-wave plasma waveguide. Here n denotes an integral number of wavelengths in the length l. At the minima of the transmission curve the helicon signal has rotated by an odd half-integral number of wavelengths and consequently interferes destructively with the leakage signal producing a minimum. In Fig. 1(b) the maxima and minima are labeled according to the number of wavelengths in the distance l.

III. WAVEGUIDE EFFECTS

It is possible to construct a dispersion relation for the helicons in a plasma waveguide from the knowledge of the number of wavelengths (i.e., of k, the propagation vector) in the bar as a function of the magnetic field. However, the infinite-medium dispersion relation given in Eq. (1) is not correct for a waveguide, and must be modified to take into account the boundaries which have been added to the plasma in order to keep the drift current to a finite value. The helicon dispersion relation,[5] for a square plasma guide with a magnetic

[4] C. C. Grimes and S. J. Buchsbaum, Phys. Rev. Letters **12**, 357 (1964).

[5] This equation may be shown by a simple plausibility argument, which assumes that helicons behave as ordinary electromagnetic waves (i.e., with a spatial dependence of $e^{i\mathbf{k}\cdot\mathbf{r}}$) which are propagating in an anisotropic medium (a magnetoactive plasma). Choosing the z axis parallel to the guide axis and B, boundary conditions require $k_x=l\pi/a$ and $k_y=m\pi/b$, where l and m are integers; and a and b are the transverse guide dimensions in the x and y directions, respectively. k_z is a continuous variable since the guide is assumed infinite in the z direction. The anisotropy of the helicon-supporting plasma may be described by the equation

$$k^2(\theta)=k_H^2/\cos\theta\equiv\omega_p^2\omega/\omega_c c^2\cos\theta,$$

where θ is the angle between the total propagation vector $k(\theta)$ and the magnetic field, which is assumed parallel to the z axis. θ is given by

$$\cos\theta=k_z/(k_x^2+k_y^2+k_z^2)^{1/2}.$$

Combining the last two equations yields

$$k_H^2=k_z[k_z^2+(k_x^2+k_y^2)]^{1/2},$$

where $k_H^2=\omega_p^2\omega/\omega_c c^2$. Using the eigenvalues of k_x and k_y given above, we obtain Eq. (3a) with $a=b$ and $l=m=1$ and with $\gamma=1$. This is similar to the dispersion relation derived and used by R. Bowers, C. Legendy, F. Rose, Phys. Rev. Letters **7**, 339 (1961); R. G. Chambers and B. K. Jones, Proc. Roy. Soc. (London) **A270**, 417 (1962) and P. Cotti, A. Quattropanie, and P. Wyder, Physik Kondensierten Materie **1**, 27 (1963). It should be emphasized that the above boundary condition only leads to an approximate solution for the dispersion relation. A more complete treatment of this problem is given by C. R. Legendy, Phys. Rev. **135**, A1713 (1964).

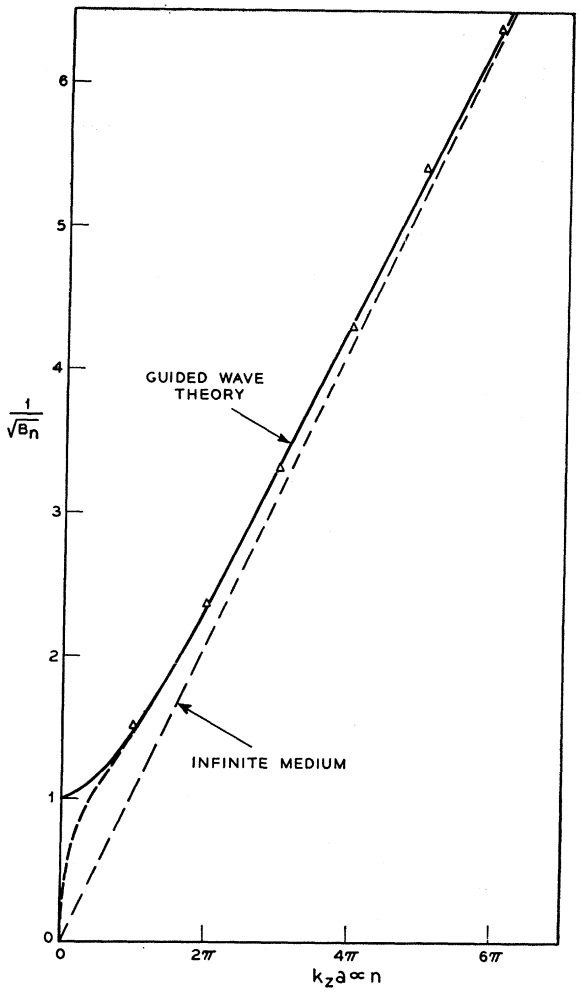

FIG. 2. Dispersion relation for the plasma-waveguide structure. The triangles are experimental values of $B_n^{-1/2}$ as a function of $k_z a$, for a frequency of 1.5 Mc/sec. The solid curve is the theoretical dispersion relation based on Eq. (3b), assuming $\gamma=1.1$. The dashed straight line is the theoretical dispersion relation for an infinite medium. The units of B_n are Wb/m².

field parallel to the guide axis, may be written, assuming $\omega_c\tau \to \infty$, approximately as

$$\omega\omega_p^2/\omega_c c^2 = k_z[k_z^2+2(\gamma\pi/a)^2]^{1/2} \qquad (3a)$$

$$\simeq k_z^2+(\gamma\pi/a)^2, \quad k_z \geq \gamma\pi/a, \qquad (3b)$$

where a is the transverse dimension of the guide, and γ is a constant depending on the mode of propagation and is of the order of unity. k_z is the component of the total propagation vector k along the guide and is the quantity measured in this experiment since $k_z=2\pi/\lambda_z = 2\pi n/l$. Equation (3a) is similar to that used by other workers[5] to interpret helicon-resonance experiments, except that in resonance k_z is assumed to possess certain eigenvalues. These are $k_z=p\pi/c$, where p is an integer, and c is the dimension of the resonance slab in the direction parallel to the magnetic field.

Figure 2 shows a comparison of the theoretical dispersion relations[6] with experimental values of $k_z a \propto n$ and $B_n^{-1/2}$ for a typical experimental configuration. The solid curve is a theoretical curve based on Eq. (3b) fitted at $k_z a=4\pi$ with $\gamma=1.1$. The dotted curve is Eq. (3a). The dashed line in Fig. 2 is the infinite medium limit $a \to \infty$, which predicts that the oscillations are periodic in $B^{-1/2}$ with a period

$$P=\Delta(B^{-1/2})=2\pi(\mu_0\omega Ne)^{-1/2}l. \qquad (4)$$

Figure 2 shows that, in regions in which we are working, Eq. (3b) is adequate for our use, even though it predicts, incorrectly, a cutoff frequency. Using a long slender bar of material with widely spaced coils ($l=7.0$ mm), we have verified the prediction of Eq. (3a) that there is no cutoff for the helicons in the plasma guide. Figure 3 shows the experimental dispersion relation for small values of $k_z a$, using this sample. This figure shows clearly the breakdown of Eq. (3b) in the region of $k_z a<\gamma\pi$.

IV. DRIFT-CURRENT EFFECT

If the drift current is added to the plasma in a waveguide Eq. (3a) and (3b) must be modified on the

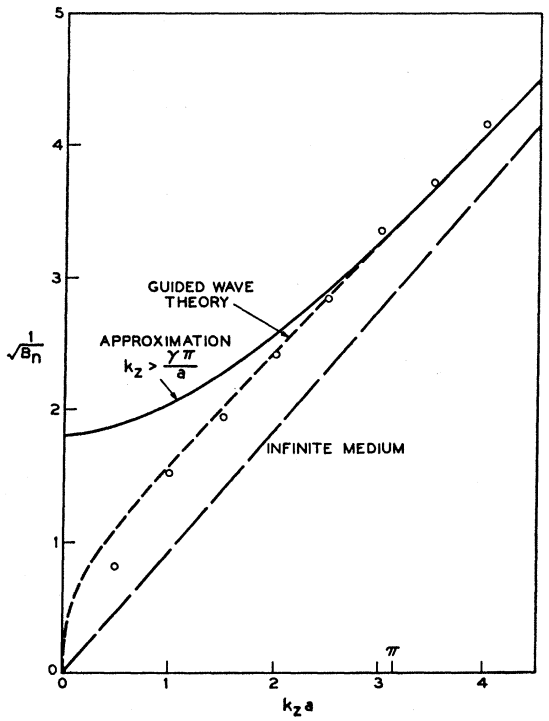

FIG. 3. Experimental and theoretical dispersion relations in the region $k_z a$ is small at a frequency of 2.0 Mc/sec in a long thin sample (N-9). The solid curve is the theoretical dispersion relation based on Eq. (3b). The dashed curve is Eq. (3a), assuming $\gamma=0.7$. The units of B_n are Wb/m².

[6] We take the liberty of calling our $(B^{-1/2},ka)$ curves "dispersion curves", since experimentally B is a more convenient variable than ω. Equation (3a) shows the results to be analogous to a $(\omega^{1/2},k)$ curve.

left-hand side to read

$$\omega\omega_p^2/\omega_c c^2(1-\mathbf{k}\cdot\mathbf{v}_D/\omega)=\omega\omega_p^2/\omega_c c^2(1-k_z v_D/\omega)$$
$$=k_z[k_z^2+2(\gamma\pi/a)^2]^{1/2} \quad (5a)$$
$$\simeq k_z^2+(\gamma\pi/a)^2. \quad (5b)$$

The effect of drift current on the real part of k_z or the guide velocity $v_z=\omega/k_z=fl/n$ is determined by measuring the change in magnetic field necessary to correct for a Doppler shift in v_z due to v_D. This measurement is accomplished by the following method, which makes optimum use of the S/N ratio inherent in narrowband detection schemes. The phase-sensitive detector is locked onto the frequency of the magnetic-field modulation signal b_{ac}, so that the output is the derivative of the curve shown in Fig. 1, thus eliminating the leakage signal. The magnetic field is adjusted to a value $B_n(0)$, so that the output of the detector is a null; i.e., n equals a half or whole integer. The output-amplifier gain may then be increased to the noise limit with no problem of remaining on scale. A dc current is then passed through the sample, which results in a shift from the null condition, due to a change in the helicon guide velocity v_z. The magnetic field is then adjusted to a new value $B_n(v_D)$ to return to the null condition. This keeps n, or equivalently the guide velocity v_z, constant. The method is entirely static, eliminating many problems associated with sweeping the field with a constant drift current or pulsing the current at constant field.

Figure 4 shows the results of measurements made in the way described above. Figure 4(a) shows the theoretical curves for the guide v_z and infinite-medium phase velocities v_H as a function of the drift current for relatively large values of drift current. This figure shows the theoretical behavior of the helicon velocity for large drift velocities ($v_D \simeq v_H$) and gives some indication of the region in which our measurements are made. The small rectangle in Fig. 4(a) is magnified and shown in Fig. 4(b). In Fig. 4(b) the theoretical guide velocity as a function of the drift velocity is determined from Eq. (5b). The drift velocity is calculated from $v_D=J/Ne$, where J is the current density and N is the electron concentration of $5.4\times10^{17}/\text{cm}^3$ for this sample. The experimental values of guide velocity are the velocities calculated from the magnetic fields adjusted to compensate for the drift current. The drift currents range from zero to $\pm 25A$, through a cross section of 3.0 mm^2. The discrepancy between theory and experiment for negative drift velocities will be discussed in a subsequent paragraph.

A more general relation between the drift velocity and the magnetic-field correction may be obtained from the condition that v_z be constant for simultaneous changes in the variables B and v_D. This condition is expressed analytically by the relation

$$dv_z=(\partial v_z/\partial v_D)dv_D+(\partial v_z/\partial B)dB=0. \quad (6)$$

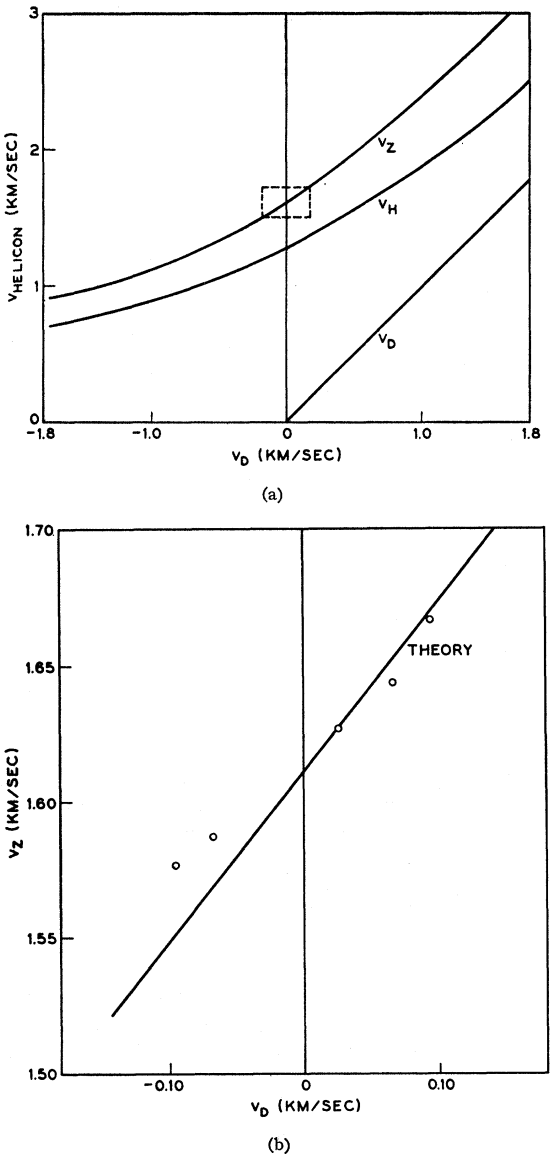

FIG. 4. (a) The theoretical guide and infinite-medium phase velocities as a function of drift velocity for sample N-3. The frequency employed is 900 kc/sec and a magnetic field of 301 gauss. (b) A magnified section of the guide-velocity curve shown in Fig. 4(a). The experimental points were taken using current densities up to 840 A/cm^2.

Using Eq. (5b) and the partial differential equation above, it may be readily shown that

$$dB/B \simeq dv_D/v_H[1-(\lambda_H/\lambda_c)^2]^{1/2}, \quad (7)$$

where $\lambda_H=2\pi v_H/\omega$, and $\lambda_c=2a/\gamma$ is analogous to a cutoff wavelength. Equation (7) is valid only when $k_z a>\gamma\pi$. Equation (7) states that, in the absence of the waveguide walls, the fractional change in the magnetic field required to compensate for the drift-current Doppler effect is just the fraction that the drift velocity is of the helicon phase velocity. However, the addition of waveguide walls reduces dB/B. This is another way

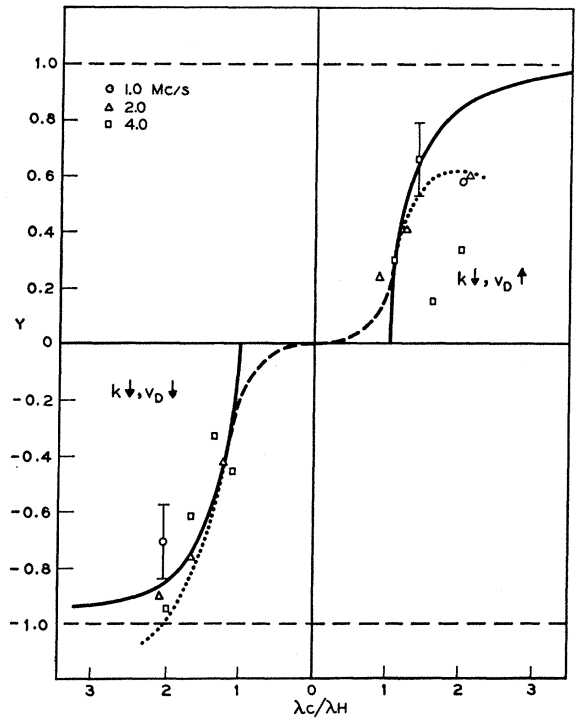

FIG. 5. $Y=(\Delta B/B)/(v_D/v_H)$ as a function of λ_c/λ_H. The experimental points are for 1.0, 2.0 and 4.0 Mc/sec. The left branch is k parallel to v_D and the right branch is k antiparallel to v_D. The solid curves are the function $(1-(\lambda_H/\lambda_c)^2)^{1/2}$. The dashed portion of the curves near the origin indicate the theoretical behavior of Y using Eq. (5a) instead of the approximate expression given by Eq. (5b). The dotted curves show the effect of the damping terms on the measurement of Y for the 2-Mc/sec data. The error bars indicate typical probable errors.

of saying that the effect of the drift current on the phase velocity has been reduced. The mechanism of this reduction is a decoupling between the $\mathbf{k}$ and $\mathbf{v}_D$ terms of Eq. (1), since $\mathbf{k}$ is no longer parallel to $\mathbf{v}_D$ in the waveguide region.

The experimental values of the ratio $Y=(\Delta B/B)/(v_D/v_H)$, as a function of λ_c/λ_H, are shown in Fig. 5. Y is the deviation from the infinite-medium helicon-drift-current interaction due to waveguide effects. It should be noted that the expression for Y is written in terms of v_H and not v_z, so that the decrease in Y from unity is due entirely to the decoupling effect. Experimentally, we measure ΔB and B. v_H, λ_H, and v_D are determined from the carrier concentration given by Eq. (4), and λ_c is an adjustable parameter. The sample is a bar of n type PbTe at 1.8°K with a concentration of 3.6×10^{17}/cc. The dimensions are $a\times b\times c=1.5\times2.0\times12$ mm^3, and the separation of the coils is $l=3.5$ mm. The solid curves of Fig. 5 are the theoretically expected term $(1-(\lambda_H/\lambda_c)^2)^{1/2}$ as a function of λ_c/λ_H. Here we have taken $\lambda_c=1.55(a+b)/2$, which is equivalent to $\gamma=1.3$. The lower-left branch of Fig. 5 are the data points for k parallel to v_D; here ΔB is negative as expected from Doppler-effect considerations. The upper-right branch, where k is antiparallel to v_D, shows the opposite shift in ΔB. The dashed line intersecting the origin shows the theoretical result obtained if Eq. (5a) were employed instead of Eq. (5b).

Part of the scatter of Fig. 5 is due to the necessity of keeping the power dissipation small (~3 W/cm^2) in order to avoid film boiling[7] of the liquid helium around the sample. (Film boiling around PbTe introduces a runaway situation with respect to the sample temperature, which destroys the sample in a fraction of a second unless the dc power is removed.) This power dissipation limits the current density to $\sim10^3$ A/cm^2; consequently, v_D is only a few percent of $v_H(\sim10^5$ cm/sec) and the measured quantity $\Delta B/B$ is still smaller, so that errors[8] are typically 10–20% full scale; i. e., $Y=1$. However, the values of Y for k antiparallel to v_D are less than those for k parallel to v_D, and the difference is outside experimental error. The asymmetry in Y is larger as λ_c/λ_H becomes larger, so that the asymmetry does not appear to be associated with wave guide effects which become smaller in this region.

An explanation for the asymmetry is found when the effect of damping is taken into account. The helicon transmission signal h (Fig. 1b), as a function of magnetic field, may be described, including collision damping, in the region $\lambda_H/\lambda_c\ll1$ by the function

$$h\sim e^{ikz}e^{-kz/2\omega_c\tau}, \tag{8}$$

where the k dependence on magnetic field is given by $k=(Ne\omega\mu_0/B)^{1/2}$. If a drift current is added, then k becomes a function of the drift velocity as well, so that

$$h\sim\exp[ik(1\pm kv_D/2\omega)z]\times\exp[-k(1\pm kv_D/2\omega)z/2\omega_c\tau], \tag{9}$$

where we have assumed $v_D\ll\omega/k$ and τ is not a function of v_D.

Equation (9) is a sinusoid enclosed in an exponential envelope. Consequently, the maximum or minimum of the damped sinusoid, when plotted as a function of magnetic field, will not be located at the same value of field as the undamped sinusoid. In principle, it is possible to take the derivative of Eq. (8) with respect to field, set it equal to zero, and solve for the zeros as a function B for the two drift-current directions to determine whether or not an asymmetry exists. In practice, the derivative of Eq. (9) is sufficiently complicated that it is convenient to solve it numerically.

---

[7] C. Nanney, Appl. Phys. Letters **1**, 71 (1962). P. C. Eastman and W. R. Datars, Cryogenics **3**, 40 (1963). Critical heat fluxes for the onset of film boiling are 0.50 W/cm^2 at 4.2°K and 3.5 W/cm^2 for $T\leq1.9$°K. The critical-heat flux is at a minimum exactly at the lambda point of helium.

[8] In general the scatter increases at the higher frequencies (e.g., the 4 Mc/sec data) since the ratio of v_D/v_H becomes smaller. This is partly the result of the helicon velocity increasing at the higher frequencies and magnetic fields. Concomitantly, the increased-longitudinal magnetoresistance at higher fields lowers the maximum current which may be used and hence v_D. On the other hand, there is a low-frequency limit determined by the condition $\omega_c\tau>1$.

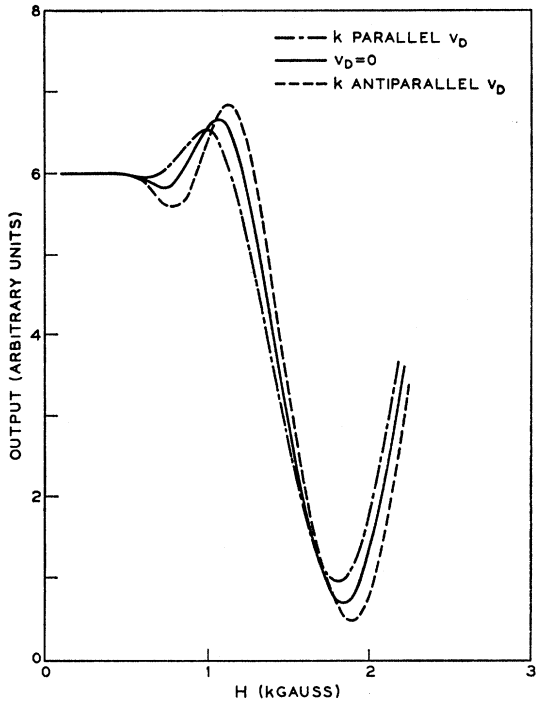

FIG. 6. Effect of drift current on helicon transmission at a frequency of 2 Mc/sec in sample N-1. The three curves are for $I=0, \pm 16A$ ($v_D=0, \pm 185$ m/sec). This shows the most damped wave appearing with the largest amplitude in the transmission curve. More structure may be seen in the region $H<0.5$ kG by increasing the gain, but here this is lost in the pen overlap.

Numerical calculations were carried out, and the results show that an asymmetry does exist in the measured magnetic-field increments ΔB for the two directions of drift current. For the calculations, the mobility was taken as 1.0×10^6 cm^2/V sec, as determined from the Hall constant and the conductivity of the sample. The results of the calculations for the 2Mc/sec, data are shown as the dotted portion of the curves in Fig. 5. This shows that the asymmetry is to be expected when damping is taken into account. This effect is not fundamental in nature, but merely an outgrowth of our inability to measure the exact wavelength (or k_z) apart from that given by the maxima and minima of the transmission curve, whose positions are determined in part by the damping.

It is worthwhile to point out that the helicon transmission given by Eq. (9) leads to a somewhat novel and, at first, contradictory result. One direction of drift current increases the damping of the wave (i.e., v_D antiparallel to k), and the other direction decreases the damping. However, as shown in the experimental transmission curve in Fig. 6, the most damped wave appears the largest in amplitude. This comes about because the real part of k is also increased by the drift current; consequently, the condition for maxima and minima requires larger magnetic fields where damping is smaller. The result is that the change in the real part of k leads to a higher field, which more than compensates the increased damping due to the increase in the imaginary part of k.

V. CONCLUSIONS

In conclusion, we have shown that a drift current does produce a Doppler-type interaction with helicons, which is in reasonably good argeement with the theory of Bok and Nozieres provided it is modified to take into account waveguide effects and if the effect of the damping is considered. The physical explanation of the waveguide effects is that in the waveguide region $\mathbf{k}$ and $\mathbf{v}_D$ become decoupled, owing to the fact that $\mathbf{k}$ is no longer parallel to $\mathbf{v}_D$ as in the infinite-medium case. This decoupling must be considered in any attempt to amplify helicon waves by means of a drift current as proposed by Bok and Nozieres,[1] since the carriers must be drifted proportionately faster than in an infinite plasma.

ACKNOWLEDGMENTS

The author wishes to acknowledge helpful discussions with D. J. Bartelink. S. J. Buchsbaum, A. G. Chynoweth, and A. Hasegawa. He wishes to thank P. H. Schmidt and J. H. Wernick for supplying the PbTe crystals used in this experiment. These experiments have benefited from the very able technical assistance of J. P. Garno.